Shivakumar I. Ranganathan
Mem. ASME
e-mail: shivakumar.ranganathan@uth.tmc.edu

Paolo Decuzzi[1]
e-mail: paolo.decuzzi@uth.tmc.edu

Lewis T. Wheeler[2]
Fellow ASME
e-mail: lwheeler@uh.edu

Mauro Ferrari[3]
e-mail: mauro.ferrari@uth.tmc.edu

Department of Nanomedicine and Biomedical Engineering,
University of Texas Health Science Center at Houston,
1825 Pressler,
Houston, TX 77030

Geometrical Anisotropy in Biphase Particle Reinforced Composites

Particle shape plays a crucial role in the design of novel reinforced composites. We introduce the notion of a geometrical anisotropy index A to characterize the particle shape and establish its relationship with the effective elastic constants of biphase composite materials. Our analysis identifies three distinct regions of A: (i) By using ovoidal particles with small A, the effective stiffness scales linearly with A for a given volume fraction α; (ii) for intermediate values of A, the use of prolate particles yield better elastic properties; and (iii) for large A, the use of oblate particles result in higher effective stiffness. Interestingly, the transition from (ii) to (iii) occurs at a critical anisotropy A^{cr} and is independent of α. [DOI: 10.1115/1.4000928]

1 Introduction

Particle reinforced composites are ubiquitous in nature yet their behavior is not completely well understood. For instance, hard nanoparticles dispersed in a much softer matrix leads to dramatic improvements in the elastic properties. The bone in vertebrate animals is an example of a natural composite where thin platelets of hydroxyapatite (5–6 nm thick and several tens of nanometers in lateral dimension) are embedded in a proteinaceous organic matrix [1]. This is also the case of dentin, the calcified tissue of teeth, where a collagen rich matrix is reinforced by calcium phosphate crystals [2]. The shells of mollusks constitute another interesting example. The abalone shell is in fact composed by stacked thin platelets of calcium carbonate (200–300 nm thick) interconnected through an organic glue [3]. Wood, too, can be considered as a natural composite with its cellulose fibrils (5–20 nm in diameter and several hundred of nanometers in length) embedded in a noncellulosic matrix [4]. Interestingly, the natural composites listed above use particles with high aspect ratios, either in the platelet or fibril form. For manmade materials, composites containing particles with small aspect ratios (spherical and ovoidal particles) were studied extensively [5]. However, dramatic improvements in mechanical properties have been again achieved by incorporating in polymeric matrix a few weight percentages of particles with large geometrical anisotropy, as in the case of exfoliated clay minerals (about 1 nm thick and 30 nm and more lateral dimension [6]) and carbon nanotubes (both in the single and multiwalled configuration [7]).

The properties of particle-filled composite materials depend on: (i) the original properties of the matrix and particle; (ii) dispersion and concentration of the particles filled in the matrix; (iii) secure bonding at the interface between the particle filler and the matrix; and (iv) on the geometrical features of the particle, in particular, the size and the shape. The scope of this article is to provide a framework using the notion of a geometrical anisotropy index to understand the effect of particle shapes on the mechanical properties of composites with polymeric matrix embedded with stiffer particles. Toward this objective, in the subsequent sections, we first briefly describe the theory used in our analysis and then introduce a new anisotropy measure to quantify the particle shape, and establish its relationship with the effective elastic constants of the material.

2 Theory

Consider a biphase composite with a matrix of stiffness $\mathbf{C}^m$, particles of stiffness $\mathbf{C}^f$, and volume fraction α. According to the effective medium (EM) theories [8], the effective stiffness may be expressed as follows:

$$\mathbf{C}^{\text{eff}} = \mathbf{C}^m + \alpha\langle(\mathbf{C}^f - \mathbf{C}^m)\hat{\mathbf{T}}\rangle \tag{1}$$

where $\langle . \rangle$ indicates the orientational averaging, and $\hat{\mathbf{T}}$ is defined as

$$\hat{\mathbf{T}} = [\mathbf{I} + \hat{\mathbf{E}}(\mathbf{C}^m)^{-1}(\mathbf{C}^f - \mathbf{C}^m)]^{-1} \tag{2}$$

with $\mathbf{I}$ being the fourth rank identity tensor and $\hat{\mathbf{E}}$ as the strain concentrator defined as follows for the equivalent poly-inclusion (EPI) and the Mori–Tanaka (MT) [9] approaches:

$$\hat{\mathbf{E}} = (1 - \alpha)\mathbf{E}(\text{EPI}) \tag{3a}$$

$$\hat{\mathbf{E}} = (1 - \alpha)\mathbf{E} + \alpha(\langle\mathbf{T}\rangle\mathbf{T}^{-1} - \mathbf{I})(\mathbf{C}^f - \mathbf{C}^m)^{-1}\mathbf{C}^m(\text{MT}) \tag{3b}$$

In the above, $\mathbf{E}$ represents the Eshelby's tensor [10,11] that accounts for the shape of the particle and the Poisson's ratio of the matrix, while $\mathbf{T} = [\mathbf{I} + \mathbf{E}(\mathbf{C}^m)^{-1}(\mathbf{C}^f - \mathbf{C}^m)]^{-1}$ represents the concentrator for the limiting case of a single anisotropic ellipsoidal particle embedded in an infinite matrix. For randomly oriented particles in an isotropic matrix, $\langle\mathbf{T}\rangle\mathbf{T}^{-1} = \mathbf{I}$, and thus, the MT and EPI theories, predict identical results. Using Eqs. (2), (3*a*), and (3*b*) in Eq. (1), the effective elastic properties of the biphase composite can be determined. Although we restrict our discussion to the EPI and MT approaches, our development can be easily extended

[1]Corresponding author. Also at Center of Bio-/Nanotechnology and Bio-/Engineering for Medicine, University of Magna Graecia, Viale Europa, LOC. Germaneto, 88100 Catanzaro, Italy.

[2]Also at Department of Mechanical Engineering, University of Houston, Engineering Building One, Houston, TX 77204.

[3]Also at Department of Experimental Therapeutics, University of Texas M.D. Anderson Cancer Center, 1515 Holcombe Boulevard, Houston, TX 77030; Department of Bioengineering, Rice University, Houston, TX 77005.

Contributed by the Applied Mechanics Division of ASME for publication in the JOURNAL OF APPLIED MECHANICS. Manuscript received August 11, 2009; final manuscript received October 9, 2009; published online April 19, 2010. Assoc. Editor: Yonggang Huang.

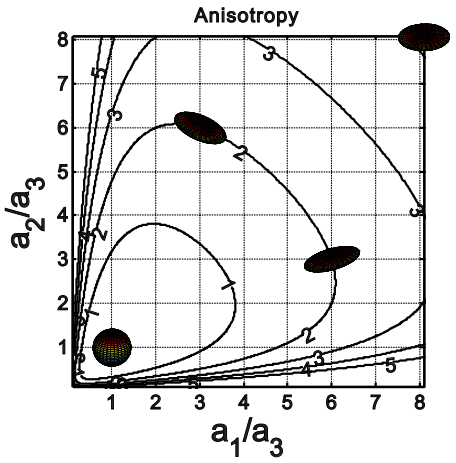

Fig. 1 Contours of constant geometric anisotropy index *A* in the (k_1, k_2) space

alongside any EM theory. We believe that the essential physics of the problem under consideration is unaffected by the choice of the EM approach used.

3 Particle Shape and Geometrical Anisotropy

Consider ellipsoidal particles (semiprincipal axis a_1, a_2, and a_3) uniformly distributed in a softer matrix. By changing the ratios $k_1=a_1/a_3$ and $k_2=a_2/a_3$, while keeping fixed $a_3=1$, different shapes for the particle can be identified, ranging from elongated prolate spheroids $(k_1,k_2 \ll 1)$ to thin oblate spheroids $(k_1,k_2 \gg 1)$, passing through the classical spherical shape $(k_1=k_2=1)$. Motivated by the definition of material anisotropy index recently proposed in Ref. [12], we introduce a parameter A to quantify the geometrical anisotropy of the particle as

$$A = 3\left(\frac{a_{AM}}{a_{HM}} - 1\right) \geq 0 \tag{4}$$

where $a_{AM}=\frac{1}{3}(a_1+a_2+a_3)$ and $a_{HM}^{-1}=\frac{1}{3}(a_1^{-1}+a_2^{-1}+a_3^{-1})$ represent the arithmetic and the inverse harmonic means of the semiprincipal axis, respectively. Rewriting Eq. (4) in terms of the ratios k_1 and k_2, it follows

$$A = \frac{1}{3}(1+k_1+k_2)(1+k_1^{-1}+k_2^{-1}) - 3 \geq 0 \tag{5}$$

The parameter A is infinitely large for a flat penny $(k_1,k_2 \to \infty)$ and for a needle $(k_1,k_2 \to 0)$, while zero is for a sphere. A can be used to quantify the departure of the particle shape from that of a sphere, thus justifying the definition of geometrical anisotropy. In Fig. 1, a contour plot for A is presented as a function of k_1 and k_2. The contours are symmetrical about the line $k_1=k_2$, and for a given volume of the particles $(k_1k_2=c)$, there are two possible choices of (k_1,k_2) resulting in the same A.

4 Discussion

Following the methodology discussed in the previous sections, the effective elastic constants can be computed as a function of the parameters k_1 and k_2, as shown in Figs. 2(*a*) and 2(*b*). The results are presented for a composite material with poly(propylene) fumarate (PPF) matrix and silicon particles. The combination of these materials is currently being used for bone reconstruction, and the material properties are listed in Table 1. The contour lines are surprisingly similar to the iso-*A* plots in Fig. 1, exhibiting the same characteristic drop shape, and are symmetrical with respect to the $k_1=k_2$ line. Moving on such a line from the spherical case $(k_1=k_2=1)$ toward larger values of $k_1(=k_2>1)$, the spheroidal particle becomes more and more oblate, and in the limit, degenerates into an infinitely thin disk (flat penny: $k_1=k_2 \to \infty$), whereas moving in the opposite direction toward smaller values of $k_1(=k_2<1)$, the spheroidal particle becomes more and more prolate, and in the limit, degenerates into an infinitely long thin cylinder (needle: $k_1=k_2 \to 0$). From the analysis of Figs. 2(*a*) and 2(*b*), it can be inferred that the elastic constants of the composite material increase as the geometry of the particle deviates from that of a sphere (i.e., as the geometrical anisotropy increases), and the absolute minimum is predicted to occur for spherical particles (geometrically isotropic). Clearly, the mechanical properties improve as α increases and as the particle becomes geometrically anisotropic. Given the striking similarity between the contours of Figs. 1 and Figs. 2(*a*) and 2(*b*), it is then intriguing to speculate that the elastic properties of the composite material could be simply derived by appropriately scaling the contours of A. To assess this point, the normalized elastic properties of the composite material are plotted in Figs. 3(*a*) and 3(*b*) as a function of A and for different α. The elastic properties are normalized with respect to those of a composite material with spherical particles $(A=0)$. The plots in Figs. 3(*a*) and 3(*b*) show a quite accurate linear relationship between the normalized elastic moduli and A. An explicit scaling expression can be derived, relating the normalized E and G to A with the general form

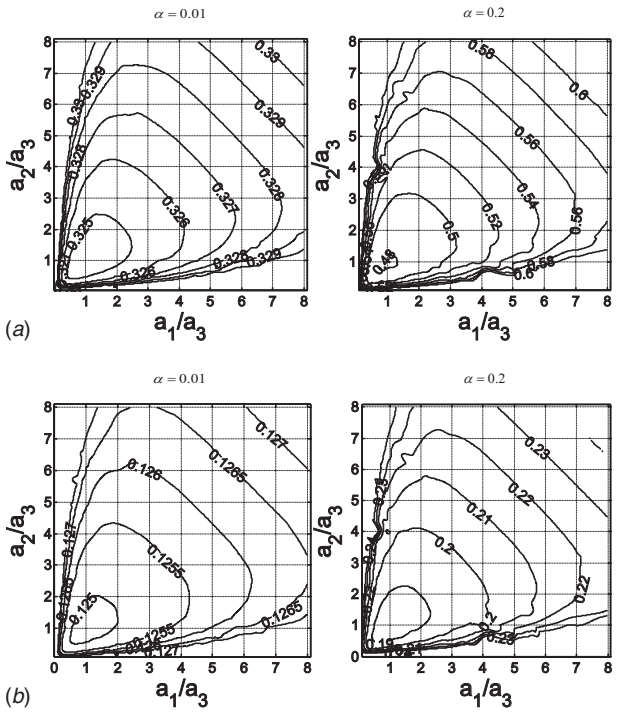

Fig. 2 (*a*) Iso-*E* (GPa) contours in the (k_1, k_2) space for $\alpha = 0.01$ and 0.2. (*b*) Iso-*G* (GPa) contours in the (k_1, k_2) space for $\alpha = 0.01$ and 0.2.

Table 1 Material properties [13]

Material	Bulk modulus K (GPa)	Shear modulus G (GPa)
PPF (matrix)	0.265	0.1223
Silicon (particle)	99.23	67.1

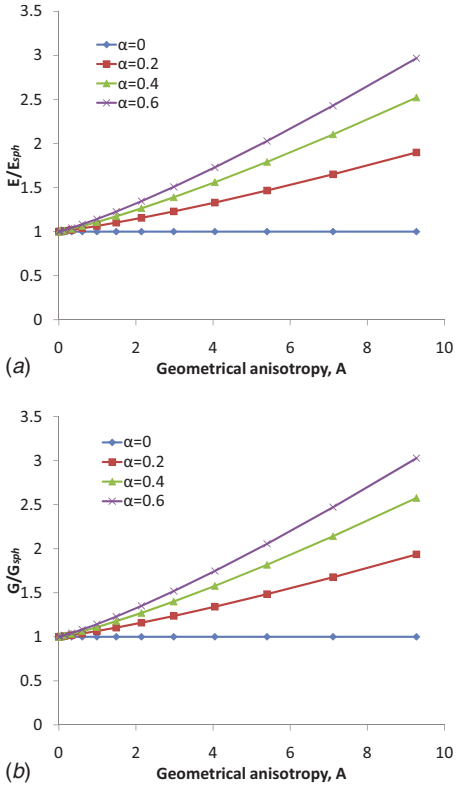

Fig. 3 (*a*) Normalized elastic moduli of the composite material as a function of *A* and α. (*b*) Normalized shear moduli of the composite material as a function of *A* and α.

$$\frac{E}{E_{\text{sph}}(\alpha)} \cong \frac{G}{G_{\text{sph}}(\alpha)} \cong g(\alpha)A + 1 \tag{6}$$

where $g(\alpha)$ represents the appropriate scaling function (slope of the lines in Figs. 3(*a*) and 3(*b*) that strongly depends on α. $E_{\text{sph}}(\alpha)$ and $G_{\text{sph}}(\alpha)$ correspond to the lower Hashin–Shtrikman bound [14,15]. The above scaling relationship implies that for $A(\leq 10)$, the differences between prolate and oblate spheroids are minimal. The results presented so far have been verified to be independent of the material combination used.

Equation (6) clearly shows a steady linear increase in the mechanical properties of the composite with the geometrical anisotropy of the particle. However, both thin oblate spheroids (platelets) and long prolate spheroids (fibril) are characterized by large values of *A*. The question naturally arise whether platelets are more effective than fibrils in improving the mechanical response of composites. This is analyzed by generating iso-contours of the prolate-oblate ratios of the shear (G_P/G_O) and Young's modulus (E_P/E_O) as a function of α and *A*, as illustrated in Figs. 4(*a*) and 4(*b*). The following distinct regions can be readily identified.

(a) For $0 \leq \log_{10}(1+A) \leq 1$, there is no distinction whether we use prolate or oblate particles.
(b) For $1 < \log_{10}(1+A) < 2.3$, the use of prolate particles give higher elastic properties.
(c) For $\log_{10}(1+A) > 2.3$, oblate particles give better elastic properties, and the contours asymptotically approach to a constant value depending on α.

The peak value occurs when $\log_{10}(1+A) \approx 1.73$, and the transition point beyond which the use of oblate particles yields higher elastic properties is essentially independent of the particle volume fraction. The transition occurs when $\log_{10}(1+A^{\text{cr}}) \approx 2.3$.

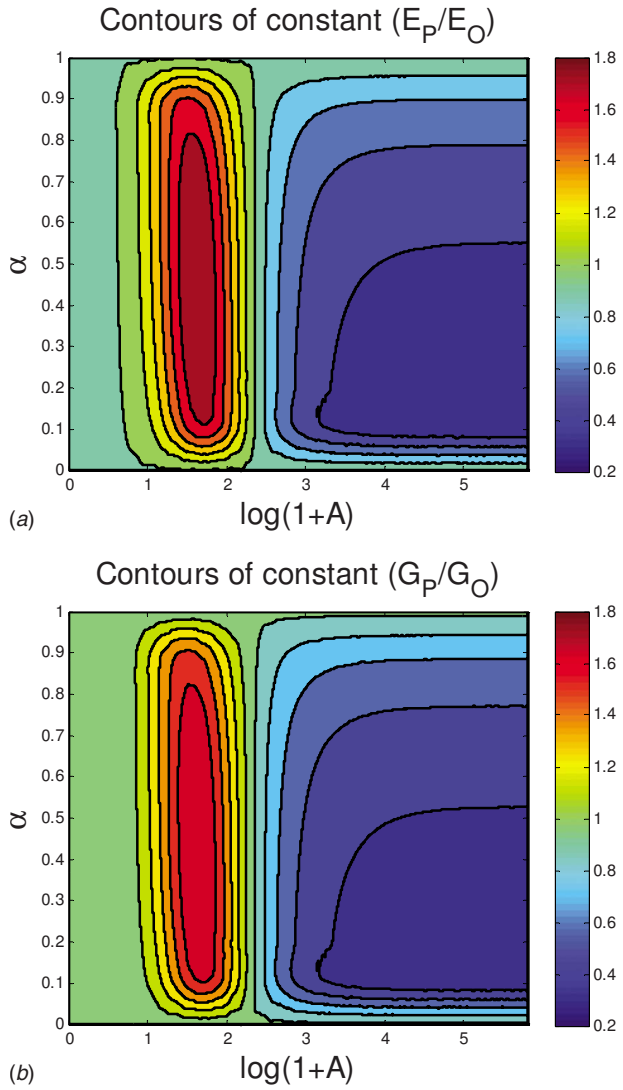

Fig. 4 (*a*) (E_P/E_O) as a function of $\log_{10}(1+A)$, and (*b*) (G_P/G_O) as a function of $\log_{10}(1+A)$

5 Conclusions

A single parameter *A* has been introduced to quantify the geometrical anisotropy of the particle. For ovoidal particles, the effective stiffness scales linearly with *A*. There is an intermediate region of *A*, for which the use of fibrils provide higher stiffness, although much higher stiffness can be obtained by using platelets with large *A* consistent with our observations in nature. On a final note, although the emphasis of this article has been on elastic properties, the notion of geometrical anisotropy is more generic and is applicable universally.

Acknowledgment

This research activity has been supported by the U.S. ARMY RDECOM ACQ CTR under Grant No. W911NF-09-1-0044, "BioNanoScaffolds (BNS) for Post-Traumatic Osteoregeneration." The authors greatly appreciate the assistance of Mr. Matthew Landry in the preparation of Figs. 2(*a*) and 2(*b*).

References

[1] Landis, W. J., 1995, "The Strength of a Calcified Tissue Depends in Part on the Molecular Structure and Organization of Its Constituent Mineral Crystals in Their Organic Matrix," Bone (N.Y.), **16**, pp. 533–544.
[2] Tesch, W., Eidelman, N., Roschger, P., Goldenberg, F., Klaushofer, K., and

Fratzl, P., 2001, "Graded Microstructure and Mechanical Properties of Human Crown Dentin," Calcif. Tissue Int., **69**, pp. 147–157.
[3] Menig, R., Meyers, M. H., Meyers, M. A., and Vecchio, K. S., 2000, "Quasi-Static and Dynamic Mechanical Response of Haliotis Rufescens (Abalone) Shells," Acta Mater., **48**, pp. 2383–2398.
[4] Ding, S. Y., and Himmel, M. E., 2006, "The Maize Primary Cell Wall Microfibril: A New Model Derived From Direct Visualization," J. Agric. Food Chem., **54**, pp. 597–606.
[5] Tjong, S. C., 2006, "Structural and Mechanical Properties of Polymer Nanocomposites," Mater. Sci. Eng. R., **53**, pp. 73–197.
[6] Giannelis, E. P., 1996, "Polymer Layered Silicate Nanocomposites," J. Adv. Mater., **8**, pp. 29–35.
[7] Xie, X. L., Mai, Y. W., and Zhou, X. P., 2005, "Dispersion and Alignment of Carbon Nanotubes in Polymer Matrix: A Review," Mater. Sci. Eng. R., **49**, pp. 89–112.
[8] Ferrari, M., 1994, "Composite Homogenization Via the Equivalent Poly-Inclusion Approach," Composites Eng., **4**, pp. 37–45.
[9] Mori, T., and Tanaka, K., 1973, "Average Stress in Matrix and Average Elastic Energy of Materials With Misfitting Inclusions," Acta Metall., **21**, pp. 571–574.
[10] Eshelby, J. D., 1957, "The Determination of the Elastic Field of an Ellipsoidal Inclusion, and Related Problems," Proc. R. Soc. London, Ser. A, **241**, pp. 376–396.
[11] Mura, T., 1987, *Micromechanics of Defects in Solids*, Kluwer Academic, Dordrecht.
[12] Ranganathan, S. I., and Ostoja-Starzewski, M., 2008, "Universal Elastic Anisotropy Index," Phys. Rev. Lett., **101**, p. 055504.
[13] Shi, X., Hudson, J. L., Spicer, P. P., Tour, J. M., Krishnamoorti, R., and Mikos, A. G., 2005, "Rheological Behaviour and Mechanical Characterization of Injectable Poly(propylene fumarate)/Single-Walled Carbon Nanotube Composites for Bone Tissue Engineering," Nanotechnology, **16**, pp. S531–S538.
[14] Hashin, Z., and Shtrikman, S., 1963, "A Variational Approach to the Theory of the Elastic Behaviour of Multiphase Materials," J. Mech. Phys. Solids, **11**, pp. 127–140.
[15] Hill, R., 1963, "Elastic Properties of Reinforced Solids: Some Theoretical Principles," J. Mech. Phys. Solids, **11**, pp. 357–372.